

This article was downloaded by:

On: 14 January 2011

Access details: *Access Details: Free Access*

Publisher *Taylor & Francis*

Informa Ltd Registered in England and Wales Registered Number: 1072954 Registered office: Mortimer House, 37-41 Mortimer Street, London W1T 3JH, UK



Molecular Simulation

Publication details, including instructions for authors and subscription information:

<http://www.informaworld.com/smpp/title~content=t713644482>

Molecular dynamics simulation of film size and vacancy defect effects on the thermal conductivities of argon thin films

Qi-Xin Liu^a; Pei-Xue Jiang^a; Heng Xiang^a

^a Key Laboratory for Thermal Science and Power Engineering of Ministry of Education, Department of Thermal Engineering, Tsinghua University, Beijing, People's Republic of China

To cite this Article Liu, Qi-Xin, Jiang, Pei-Xue and Xiang, Heng (2008) 'Molecular dynamics simulation of film size and vacancy defect effects on the thermal conductivities of argon thin films', *Molecular Simulation*, 34: 6, 645 – 650

To link to this Article: DOI: 10.1080/08927020802036047

URL: <http://dx.doi.org/10.1080/08927020802036047>

PLEASE SCROLL DOWN FOR ARTICLE

Full terms and conditions of use: <http://www.informaworld.com/terms-and-conditions-of-access.pdf>

This article may be used for research, teaching and private study purposes. Any substantial or systematic reproduction, re-distribution, re-selling, loan or sub-licensing, systematic supply or distribution in any form to anyone is expressly forbidden.

The publisher does not give any warranty express or implied or make any representation that the contents will be complete or accurate or up to date. The accuracy of any instructions, formulae and drug doses should be independently verified with primary sources. The publisher shall not be liable for any loss, actions, claims, proceedings, demand or costs or damages whatsoever or howsoever caused arising directly or indirectly in connection with or arising out of the use of this material.

Molecular dynamics simulation of film size and vacancy defect effects on the thermal conductivities of argon thin films

Qi-Xin Liu, Pei-Xue Jiang* and Heng Xiang

Key Laboratory for Thermal Science and Power Engineering of Ministry of Education, Department of Thermal Engineering, Tsinghua University, Beijing, People's Republic of China

(Received 30 November 2007; in revised form 24 January 2008; final version received 5 March 2008)

It is well known that there is a size effect for the thermal conductivity of thin films and that vacancy defects in film reduce the film's thermal conduction. In this paper, the film size and vacancy defect effects on the thermal conductivities of argon thin films were studied by molecular dynamics simulations. The results show the existence of phonon boundary scattering. The results also confirm that the theoretical model based on the Boltzmann equation can accurately model the thermal conduction of thin argon films. Both the theoretical and MD results illustrate that, although, both the defect and the thickness of the thin film deduce the thermal conductivity, their physical mechanisms differ.

Keywords: molecular dynamics simulation; size effect; vacancy; thermal conductivity

1. Introduction

Solid films with characteristic dimensions from tens to hundreds of nanometers are now key components of integrated-circuit and quantum-well lasers. For nanoscale films, the size is comparable to the mean free path of the phonons, so their thermal properties are affected by the system size. Therefore, the thermal characteristics of microscale and nanoscale films have been a key focus of international heat transfer research in the past two decades [1,2]. Measurements of thin films have shown that such materials display markedly lower thermal conductivities than their bulk counterparts. Experimental measurements have been supplemented by molecular dynamics simulations as a useful method that simulates the thermal conductivities of thin films by simultaneously solving the equations of motion for the system. The molecular dynamics methods are based on Newton's law, so the thermal conduction caused by phonons can be simulated. The MD simulations of thermal conductivities of argon thin films have been reported [3,4]. These simulations have shown that the thermal conductivities of argon nanoscale films are lower than the bulk value and that they depend on the film thickness. This phenomenon is explained as the decrease of the argon's phonon mean free path due to boundary scattering.

Real crystals always contain defects, such as impurities, vacancies and dislocations which reduce the thermal conductivity. MD simulations can also simulate the thermal conductivities of films with defects.

Several MD studies [5,6] have analysed the effects of defects on the thermal conductivity, but these studies all focused on the properties of the bulk materials. Liu et al. [7] reported on MD simulations about the effects of vacancies on nanoscale thin film thermal conductivities. We found that for nanoscale films, the defects also reduce the film's thermal conductivity with the thermal conductivity reduced by the same percentage for a given vacancy concentration.

The solid thermal conductivity can be analysed theoretically using the kinetic theory of phonon gases with the thermal conductivity given by

$$k = \frac{1}{3} c_v \bar{v}^2 \tau, \quad (1)$$

where c_v is the specific heat per unit volume, \bar{v} is the mean speed of sound and τ is the phonon's mean free time between phonon scattering events. Various studies [8–10] have analysed the thermal conductivity of solid, but have only focused on the bulk value.

In this paper, molecular dynamics simulation are used to further study the film size and vacancy defect effects on the thermal conductivities of nanoscale films with the results compared to a theoretical analysis based on the Boltzmann equation.

2. MD simulation models

The NEMD method was used to simulate the thermal conductivity of argon thin films. The model illustrated in

*Corresponding author. Email: jiangpx@tsinghua.edu.cn

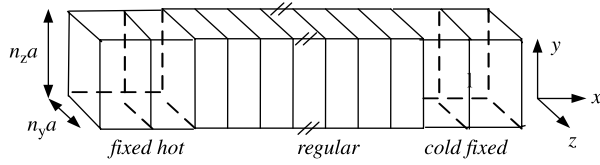


Figure 1. MD simulation model.

Figure 1 shows a cross-section of the film, along the thickness direction. In the cross-plane direction, the x -direction, each atom is assigned a type according to its spatial position as 'fixed', 'hot', 'regular' or 'cold'. The fixed atoms are stationary during the whole simulation and serve as adiabatic boundary conditions. The 'hot' and 'cold' atoms are the temperature control boundary conditions, where the velocities of each atom are controlled to maintain the desired temperature. Due to the temperature control in the 'hot' and 'cold' sections and the fixed atoms at the two ends of the film, the momentum of the total film may be not conserved, however, the momentum conservation is not a necessary condition in the NEMD method to calculate the thermal conductivity [11]. In the regular part, besides the LJ potential mode, no special control is performed to the atoms. The LJ potential is written as

$$\phi(r_{i,j}) = 4\epsilon \left[\left(\frac{\delta}{r_{i,j}} \right)^{12} - \left(\frac{\delta}{r_{i,j}} \right)^6 \right], \quad (2)$$

where ϵ is the well-depth parameter, δ is the equilibrium separation parameter and $r_{i,j}$ is the distance between two atoms. Only the neighbours of an atom within a specified cutoff radius, 2.6δ LJ, are included in the force calculations because, far away atoms have negligible effect on the total force. The model cross-section has 6×6 lattice layers. Periodic boundary conditions are used in the other two directions. The film temperature distribution was obtained by dividing the entire film into layers along the x -direction. The number of the layers depends on the film thickness. In this paper, the temperature of each layer was calculated using the formula,

$$T = \frac{\sum_{i=1}^N m_i v_i^2}{3Nk_B}, \quad (3)$$

where N is the number of atoms in the layer. The heat flux was calculated from the change in the kinetic energy of the hot and cold atoms during each simulation time step,

$$\Delta E = \pm \frac{1}{2} m \sum (v_{\text{old}}^2 - v_{\text{new}}^2). \quad (4)$$

The minus sign is for the higher temperature boundary, while the plus sign is for the lower temperature boundary. Based on the Fourier law, the thermal conductivity of the argon film is:

$$k = \frac{\Delta E_{\text{hot}} + \Delta E_{\text{cold}}}{2\tau A |\nabla T|}, \quad (5)$$

where τ is the simulation step time, A is the cross-sectional area and $|\nabla T|$ is the absolute value of the temperature gradient in the cross-plane direction.

3. MD simulation results

3.1 Pure argon films

In this study of pure argon films, the mean temperature of the simulated films was 45 K, with the higher temperature end at 55 K and the lower end at 35 K. A series of MD simulations was conducted to study the size effect on the thermal conductivity of argon thin films. The simulated film thicknesses ranged from 10 to >100 nm. Figure 2 shows the variation of the thermal conductivity with the film thickness. The thermal conductivity increases with thickness with the maximum simulated value exceeding the bulk value. For thinner films, the thermal conductivity increased rapidly with thickness. For example, from 10 to 50 nm, the thermal conductivity increases by nearly 0.1 W/m K. However, from 50 to 100 nm, the thermal conductivity increases by only 0.05 W/m K. This trend shows that at different thickness ranges, the film's thickness has different effects on the thermal conduction. When the film thickness is greater than 80 nm, the thermal conductivity of the film is slightly larger than the thermal conductivity of bulk argon at the same temperature [12].

3.2 Films with vacancy defects

Real films always contain defects including isotopes, vacancies and dislocations which reduce the phonon heat

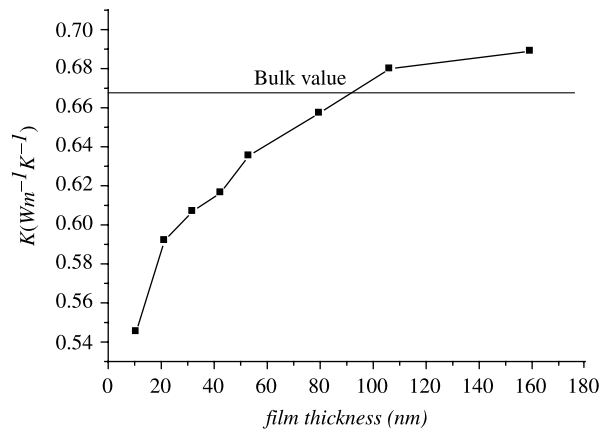


Figure 2. Thermal conductivity of argon films at 45 K.

transfer. In this paper, the vacancy defect effects on the film's thermal conductivity were studied using vacancies formed by randomly removing different selected number of atoms from the perfect FCC lattice to model vacancy densities. Simulations were done for thin argon films at both 40 and 45 K.

The thermal conductivity of 15 nm thick argon films at 40 and 45 K with vacancy densities ranging from 0.2 to 1.5% are shown in Figure 3. The results show that the vacancies significantly affect the thermal conductivity of the argon thin films. For the same film thickness, increased vacancy densities reduce the thermal conductivity. Due to the different pure film thermal conductivities at different temperatures, the thermal conductivity of the film at 40 K is larger than that at 45 K with the same vacancy density. Figure 4 shows that the thermal conductivities of 25.5 nm thick, argon films at 40 and 45 K also decrease as the vacancy increase as seen in Figure 3.

4. Analysis of the simulation results

4.1 Analysis model

In a solid, the phonon's movements are affected by various scattering process including: the normal three-phonon process, impurity scattering, the Umklapp process and boundary scattering. These phonon scattering processes can be assumed to be represented by frequency-dependent relaxation time. Therefore, these four scattering process can be described as the normal three-phonon process, whose relaxation time is proportional to $(\omega^2 T^3)^{-1}$ [9], impurity scattering whose relaxation time is proportional to ω^{-4} [9], the Umklapp process, whose relaxation time is proportional to $(e^{-\Theta/aT} \omega^2 T^3)^{-1}$ [9] and boundary scattering which describes the phonon scattering at a boundary. For nanoscale systems, the boundary scattering relaxation

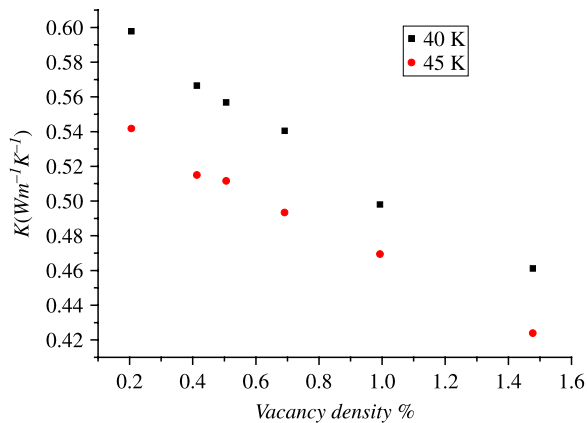


Figure 3. Thermal conductivity of 15 nm thick argon films with different vacancy densities at 40 and 45 K.

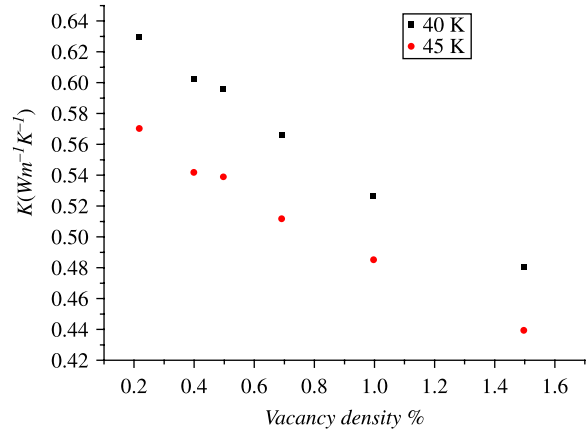


Figure 4. Thermal conductivities of 25 nm thick argon film with different vacancy densities at 40 and 45 K.

time is assumed as $(v(1-s)/L)^{-1}$, where v is the velocity of sound, L is the film thickness and s is the proportion of phonons with specular scattering [13], $1-s$ is the proportion of phonons scattered by the boundary. The lattice thermal conductivity based on the Boltzmann equation can be written as [9]:

$$\lambda = \frac{k_B}{2\pi^2 c} (I_1 + \beta I_2), \quad (6)$$

where

$$I_1 = \int_0^{k_B \Theta / \hbar} \tau_c \frac{\hbar^2 \omega^4}{k_B^2 T^2} \frac{e^{\hbar \omega / k_B T}}{(e^{\hbar \omega / k_B T} - 1)^2} d\omega, \quad (7)$$

and

$$I_2 = \int_0^{k_B \Theta / \hbar} \frac{\tau_c}{\tau_N} \frac{\hbar^2 \omega^4}{k_B^2 T^2} \frac{e^{\hbar \omega / k_B T}}{(e^{\hbar \omega / k_B T} - 1)^2} d\omega, \quad (8)$$

$$\beta = \frac{\int_0^{\Theta/T} \frac{\tau_c}{\tau_N} \frac{e^x}{(e^x - 1)^2} x^4 dx}{\int_0^{\Theta/T} \frac{1}{\tau_N} \left(1 - \frac{\tau_c}{\tau_N}\right) \frac{e^x}{(e^x - 1)^2} x^4 dx}, \quad (9)$$

where k_B is the Boltzmann constant and Θ is the Debye temperature, which is 92 K for argon. τ_N and τ_C are defined as follow:

$$\tau_N^{-1} = B_2 T^3 \omega^2, \quad (10)$$

$$\tau_C^{-1} = A \omega^4 + (B_1 + B_2) T^3 \omega^2 + (1-s)v/L. \quad (11)$$

The coefficient of A , B_1 , B_2 and s must be determined to obtain the thermal conductivity.

In pure bulk materials, normal and Umklapp processes dominate, while boundary and defect scattering processes contribute little to the thermal resistance. Thus, B_1 and B_2 can be obtained from experimental data [12] for the pure bulk argon by neglecting the boundary and

defect scattering terms in Equation (11). \bar{v} [14] and ω_D can also be calculated from data for bulk argon. After getting the parameters B_1 and B_2 , the unknown parameter s can be determined from MD simulation of the thermal conductivity of argon thin films at one thickness, for example, the 26.52 nm result is used here. Then, MD simulation results for films with a given vacancy density can be used to determine A . After these coefficients are known, the thermal conductivity of argon thin films can be predicted for various thicknesses or vacancy densities for comparison with the MD simulation results.

4.2 Analysis results for pure films

The values of B_1 and B_2 for argon at 40 K are 5.205 and $8.004 \times 10^{-20} \text{ s deg}^3$. The value of s for a 26.52 nm argon film at 40 K is 0.855. The thermal conductivities of pure argon thin film at other thickness at 40 and 45 K predicted by the model are illustrated in Figures 5 and 6. From Figure 5, the thermal conductivity predicted by the model also increases with increasing film thickness. The differences between the model predictions and the MD results vary with the film thickness. The largest difference of 6.5% occurs when the film is about 80 nm thick. It is seen from Figure 6, that like the argon film at 40 K, the largest difference between the model predictions and the MD results occurs for the thickest film. The MD results show that when the film thickness is about 100 nm, the thermal conductivity of the film approaches that of the bulk, which means that for films at such thicknesses the boundary scattering can be neglected and s for the boundary scattering effect should approach 1. Thus, the larger difference between the MD simulations and the model predictions can be explained as an underestimation of the proportion of phonons whose

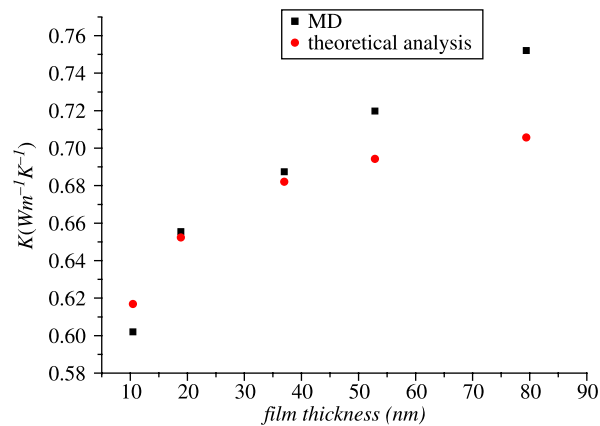


Figure 5. Thermal conductivities of pure argon thin films with different thicknesses at 40 K, model predictions with $s = 0.855$ and MD results.

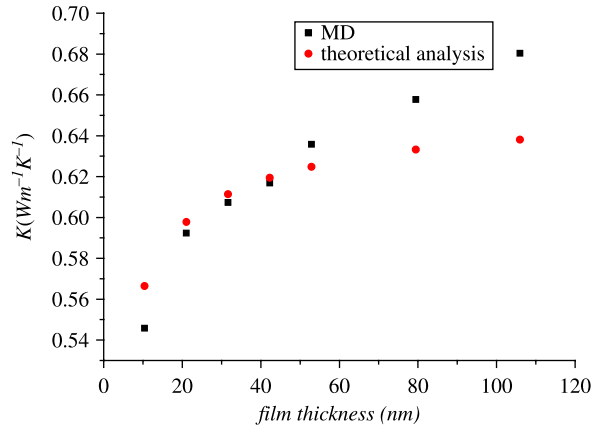


Figure 6. Thermal conductivities of pure argon thin films with different thicknesses at 45 K, model predictions with $s = 0.855$ and MD results.

boundary reflections are specular, when s is set to 0.855. For pure argon films thinner than 20 nm, the model predictions at both 40 and 45 K are larger than the MD results, because the $s = 0.855$ underestimates the boundary scattering, which becomes stronger as the film become thinner. In fact, the value of s which exactly reproduces the film thermal conductivity predicted by MD for various thicknesses depends on the film thickness because the different film thicknesses cause different boundary scattering intensities. By fitting the model to the MD results the relationship between s and the film thickness at 45 K is:

$$s = 0.78509 + 0.00192l - 1.2414 \times 10^{-5}l^2 - 1.04165 \times 10^{-7}l^3, \quad (12)$$

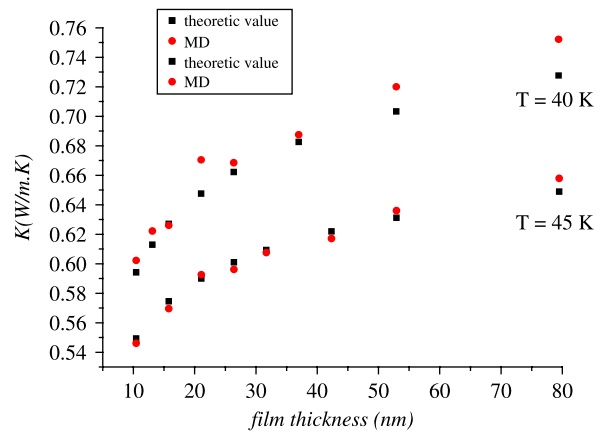


Figure 7. Thermal conductivities of pure argon thin films with various thicknesses at 40 and 45 K from model predictions with s based on Equation 12 and MD predictions.

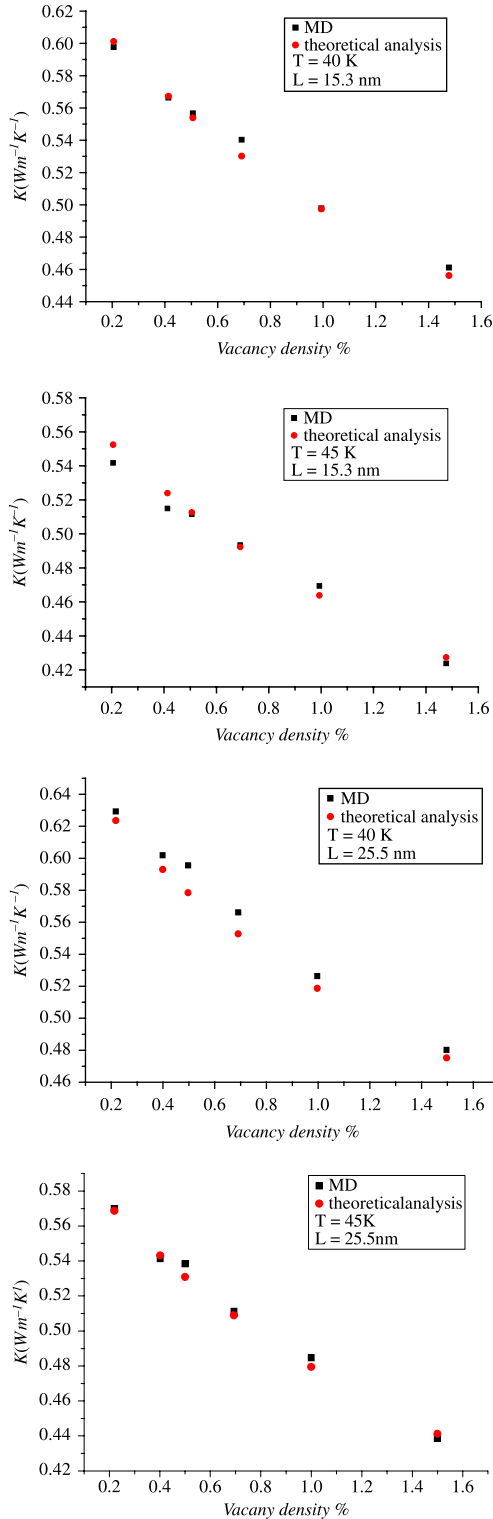


Figure 8. Thermal conductivities of argon thin films with different vacancy densities as predicted by the MD simulation and theoretical analysis.

where l is in nanometer. Figure 7 compares the theoretical predictions for the thermal conductivity for argon thin films at 40 and 45 K using the value of s from Equation 12

with the MD results. The theoretical predictions agree well with the MD results at each film thickness including both thinner and thicker films.

4.3 Theoretic analysis results for films with vacancy defects

The scattering time due to point defects can be theoretically expressed as $\tau_p^{-1} = A\omega^4$ with [15,16]:

$$A = \frac{V_0}{4\pi\bar{v}^3} \sum_i f_i \left[1 - \left(\frac{M_i}{M} \right) \right]^2, \quad (13)$$

where f_i is the defect concentration, M_i is the defect mass and V_0 is the volume of one atom. A can also be determined from the MD results of argon film with a certain vacancy concentration. The MD simulation results for 15.3 nm argon film with 0.02% vacancy defects at 40 K were used to calculate A as 2.964×10^{-39} times the vacancy density. Then the vacancy density, film thickness and the already obtained parameter B_1 , B_2 and s were used in Equations (6)–(11), to predict the thermal conductivities of argon thin films with different defect densities. The thermal conductivities predicted by the theoretical models and the MD simulations are shown in Figure 8. The thermal conductivities predicted by the analytical model agree well with the MD results for films with different vacancy densities and different thickness at both 40 and 45 K. Thus, this analytical model can accurately depict the vacancy defect effect on the argon thin film thermal conductivity. In addition, although, both the vacancy defects and the size effects reduce the thermal conductivity of thin films, the mechanism by which increased vacancy defect reduce the thermal conductivity is by their mechanisms are different. Because the defect scattering time is phonon frequency's quadruplicate proportional, the boundary scattering time is related to the system's size.

5. Conclusions

The thermal conductivities of argon thin films were calculated to investigate the size effect and the vacancy defects effect on the argon thin film thermal conductivity using MD simulations. The MD results show the film thickness affects the thermal conductivity of argon thin films and how the vacancy defects reduce the thermal conductivity. This paper also shows that the theoretical analysis based on the Boltzmann equation can predict the thermal conductivities of argon thin films. The theoretical models show that although, both defects and the thickness of thin films affect the thermal conductivity, their physical mechanisms differ.

Acknowledgements

The project was supported by the National Natural Science Foundation of China (No. 50676047) and the Tsinghua Basic Research Foundation (No. JCpy2005049).

References

- [1] C.L. Tien, and G. Chen, *Challenges in microscale conductive and radiative heat transfer*, J. Heat Transfer 116(4) (1994), pp. 799–807.
- [2] F.C. Chou, J.R. Lukes, and X.G. Liang, *Molecular dynamics in microscale thermophysical engineering*, Annu. Rev. Heat Transfer 10 (1999), pp. 141–176.
- [3] J.R. Lukes, D.Y. Li, X.G. Liang, and C.L. Tien, *Molecular dynamics study of solid thin-film thermal conductivity*, J. Heat Transfer 122 (2000), pp. 536–543.
- [4] P. Chantrenne and J.L. Barat, *Finite size effects in determination of thermal conductivities: comparing molecular dynamics results with simple models*, J. Heat Transfer 126 (2004), pp. 577–585.
- [5] Y. Chen, J.R. Lukes, D. Li, J. Yang, and Y. Wu, *Thermal expansion and impurity effects on lattice thermal conductivity of solid argon*, J. Chem. Phys. 120 (2004), pp. 3841–3846.
- [6] J. Che, T. Cagin, W. Deng, and W.A. Goddard, *Thermal conductivity of diamond and related materials from molecular dynamics simulations*, J. Chem. Phys. 113 (2000), pp. 6888–6900.
- [7] Q.-X. Liu, P.-X. Jiang, and H. Xiang, *Molecular dynamics study of the thermal conductivity of nanoscale argon films*, Mol. Simul. 32 (2006), pp. 645–649.
- [8] M.G. Holland, *Analysis of lattice thermal conductivity*, Phys. Rev. 132 (1963), pp. 2461–2471.
- [9] J. Callaway, *Model for lattice thermal conductivity at low temperatures*, Phys. Rev. 113 (1959), pp. 1046–1051.
- [10] B.K. Agrawal and G.S. Verma, *Lattice thermal conductivity at low temperatures*, Phys. Rev. 126 (1962), pp. 24–29.
- [11] Z.-X. Huang and Z.-A. Tang, *Evaluation of momentum conservation influence in non-equilibrium molecular dynamics methods to compute thermal conductivity*, Physica B. 373 (2006), pp. 291–296.
- [12] D.K. Christen and G.L. Pollack, *Thermal conductivity of solid argon*, Phys. Rev. B 12 (1975), pp. 3380–3391.
- [13] J. Zou and A. Balandin, *Phonon heat transfer in a semiconductor nanowire*, J. Appl. Phys. 89 (2001), pp. 2932–2938.
- [14] G.J. Keeler and D.N. Batchelder, *Measurement of the elastic constants of argon from 3 to 77 K*, J. Phys. C: Solid State Phys. 3 (1970), pp. 510–522.
- [15] M.G. Holland, *Analysis of lattice thermal conductivity*, Phys. Rev. 132 (1963), pp. 246–261.
- [16] B.K. Agrawal and G.S. Verma, *Lattice thermal conductivity at low temperatures*, Phys. Rev. 126 (1962), pp. 24–29.